Dynamic Assessment of Shear Connectors in Composite Bridges with Ambient Vibration Measurements

Jun Li[1,*], Hong Hao[1] and Hong-Ping Zhu[2]

[1]Department of Civil Engineering, School of Civil and Mechanical Engineering, Curtin University, Bentley, WA6102, Australia
[2]School of Civil Engineering and Mechanics, Huazhong University of Science and Technology, Wuhan, China

(Received: 29 January 2013; Received revised form: 22 July 2013; Accepted: 14 January 2014)

Abstract: Shear connectors are normally used in composite bridges, such as slab-on-girder structures, to link the slab and girder together. Damage of shear connectors will result in shear slippage between slab and girder, which significantly reduces the load-carrying capacity of the bridge. Routine visual inspection is not able to detect conditions of shear connectors because they are buried inside the structure. This paper proposes a dynamic damage detection approach based on wavelet packet energy of cross-correlation functions from ambient vibration measurements to identify the damage of shear connectors in slab-on-girder bridges. Measured acceleration responses on the slab and corresponding girder locations under ambient vibrations are used to compute the cross-correlation functions. Wavelet packet decompositions of cross-correlation functions from the undamaged and damaged structures are performed and the percentage of wavelet packet energy in selected frequency bandwidths to the total wavelet packet energy is used to calculate the damage index. Numerical and experimental studies on a composite bridge with a concrete slab supported by two steel girders are conducted to validate the proposed approach and investigate its performance and robustness with noisy measured responses. It is demonstrated that the introduced damage of shear connectors can be identified accurately and efficiently.

Key words: damage detection, shear connector, cross-correlation function, wavelet packet energy, composite bridge, ambient vibration.

1. INTRODUCTION

Many bridges are built as the slab-on-girder structures. The concrete slab is supported by the concrete or steel girders, and stirrups are embedded in the girders and cast into the slab as shear connectors to link the slab and girders together. The shear connection between slab and girders in composite structures subjects to the major consequences of stress, overloading and fatigue, especially for large structures such as bridge decks. It follows that damages usually involve a deterioration or break of the shear connection in some regions of the structure, causing a decrease of the overall rigidity of the composite structure and a reduction of its ultimate resistance (Dilena and Morassi 2004). Damage of shear connectors will result in shear slippage between the slab and girder, which significantly reduces the load-carrying capacity of the bridge. Condition assessment of shear connectors is of great interest and important to evaluate the structural integrity in health monitoring of slab-on-girder structures. Dilena and Morassi (2003) presented the modal analysis results with damage in the shear connection of steel-concrete composite

*Corresponding author. Email address: junli@curtin.edu.au/LI.Jun@connect.polyu.hk; Fax:+61-8-9266-2681; Tel: +61-8-9266-5140.

structures. Frequency shifts and changes in node positions of vibration modes are used for damage detection. Xia *et al.* (2007) proposed a local detection method by directly comparing the frequency response functions of simultaneously measured vibrations on the slab and girder. It has been found that the local method would give better identification results than global methods, since the global modal information may not be sensitive to the local damage of shear connectors. The proposed local detection approach is extended to assess the integrity condition of shear connectors in real composite bridges with in-field testing data (Xia *et al.* 2008). Recently, wavelet based Kullback-Leibler distance (Zhu *et al.* 2012) and wavelet packet energy (Ren *et al.* 2008) have also been proposed for damage identification of shear connectors. Hammer input excitation is used in the abovementioned studies to excite the structure, and it is usually measured together with the acceleration responses on the structure for identification in most studies. Liu and De Roeck (2009) proposed a local condition assessment approach to identify the damage location of shear connectors by using the modal curvature and wavelet transform modulus maxima. Modal strain were measured and used for identification.

Vibration based condition monitoring refers to the use of in situ non-destructive sensing and analysis of system characteristics whether in the frequency, modal or time domains for the purpose of detecting changes, which may indicate damage or degradation. Generally, vibration-based damage detection methods could be classified into non-model based (direct correlation) and model-based (model updating). Non-model based methods compare or correlate the measured structural dynamic characteristics from the undamaged and damaged structures for identification, while model-based methods use the iterative finite element model updating to make the analytical and measured structural vibration properties as close as possible. One major difficulty of model-based methods is that an initial accurate finite element model of undamaged structure is required for the identification, which is usually not available in practice. Many sources of uncertainties that would be introduced into the structure during their construction and service stages make it not easy to obtain an accurate finite element model that represents the intact condition of the structure as the basis of model updating for structural damage identification.

A structure can be considered as a dynamic system with stiffness, mass and damping components. Once some damages occur in the structure, the structural physical properties will change, and modal parameters of the structure will also change. Therefore, the changes in the structural vibration characteristics between the undamaged and damaged states, such as natural frequencies (Salawu 1997), mode shapes (Fryba and Pirner 2001), mode shape curvature (Hamey *et al.* 2004), flexibility (Bernal and Gunes 2004), modal strain energy (Shi *et al.* 2000), frequency response function (Samali *et al.* 2012), etc., can be used to indicate the existence of damage and to identify the location and even severity of damage. The extension of system identification methods to ambient vibration cases, in which input excitations can not be measured, is receiving more attentions. Non-model based output only system identification from ambient vibration measurements is conducted to identify the modal information, such as frequencies, mode shapes and damping ratios (Brownjohn *et al.* 1992; Wu *et al.* 2012; De Roeck *et al.* 2000). The real structures under operational conditions are only excited by random excitations from unregulated traffic, wind, flowing water and ground-transmitted vibrations. Many studies on damage identification methods with ambient vibration measurements are conducted recently (Yuen and Katafygiotis 2003; Lee and Yun 2006; Duan *et al.* 2007). They need both the monitored data from the healthy and unhealthy structures for a comparison with the dynamic system characteristics. Attention needs to be paid on the condition assessment of composite bridges with dynamic ambient vibration measurements directly, such as acceleration response data.

This paper proposes a dynamic condition assessment approach based on wavelet packet energy of cross-correlation functions from ambient vibration measurements to identify the damage of shear connectors in slab-on-girder bridges. Measured acceleration responses on the slab and corresponding girder locations under ambient vibrations are used to compute the cross-correlation functions. Wavelet packet decompositions of cross-correlation functions from the undamaged and damaged structures are performed and the percentage of wavelet packet energy in selected frequency bandwidths to the total wavelet packet energy is used to calculate the damage index. Numerical and experimental studies on a composite bridge model with a concrete slab supported by two steel girders are conducted to validate the proposed approach and investigate its performance and robustness with noisy measured responses.

2. DAMAGE DETECTION WITH EXISTING METHODS

In order to demonstrate the reliability and advantage of the proposed damage detection method, several commonly used vibration-based damage detection methods using global modal information are used for a comparison with the proposed method and these methods are briefly reviewed here.

2.1. Damage Detection of Shear Connectors with Modal Information

Coordinate Modal Assurance Criteria (COMAC) describes the correlation of mode shapes with respect to an individual point over all the modes. For point q, the COMAC is defined as (Lieven and Ewins 1988)

$$\mathrm{COMAC}\left(\phi^u, \phi^d, q\right) = \frac{\left(\sum_{i=1}^{nm}\left|\left(\phi_i^u\right)_q\left(\phi_i^d\right)_q\right|\right)^2}{\left(\sum_{i=1}^{nm}\left(\phi_i^u\right)_q^2\right)\left(\sum_{i=1}^{nm}\left(\phi_i^d\right)_q^2\right)} \tag{1}$$

where ϕ^u and ϕ^d are the structural mode shapes in the undamaged and damaged states, $(\phi_i^u)_q$ and $(\phi_i^d)_q$ represent the ith mode shape values at point q from the undamaged and damaged structures and nm is the number of mode shapes involved in the COMAC computation. Normally a low COMAC value indicates a worse correlation between two mode shapes and possible existence of the damage around the point.

2.2. Modal Flexibility

The modal flexibility matrix can be estimated from the measured modal frequencies and normalized mode shapes (Pandey and Biswas 1994) as

$$F = \sum_i^{nm} \frac{1}{\omega_i^2}\left\{\phi_i\right\}\left\{\phi_i\right\}^T \tag{2}$$

where F is the flexibility matrix, ω_i is the ith modal frequency, ϕ_i is the ith mode shape.

If two sets of measurements, one for the intact structure and another for the damaged structure, are taken and modal parameters are identified from the measurements. Then the flexibility matrix for the two cases can be obtained and change in the flexibility matrix Δ can be calculated as

$$\Delta = F_i - F_d \tag{3}$$

where, F_i and F_d are the flexibility matrices for the intact and damaged cases, respectively. For each measurement location j, let $\bar{\delta}_j$ be the maximum absolute value of the elements in the corresponding column of Δ, i.e.

$$\bar{\delta}_j = \max_i \left|\delta_{ij}\right| \tag{4}$$

where δ_{ij} are elements of the jth column of Δ. To detect and locate damage in a structure, the quantity $\bar{\delta}_j$ is used as the measure of change of flexibility for each measurement location.

3. THEORETICAL BACKGROUND

The formulation of cross-correlation function between two time-domain responses from the structure under ambient vibration will be introduced. The wavelet packet energy of cross-correlation functions in the undamaged and damaged states in selected frequency bandwidths will be used to conduct the damage identification of shear connectors in slab-on-girder structures.

3.1. Cross-Correlation Function of Two Time-Domain Responses

The general equation of motion of a damped structure with n degrees-of-freedom (DOFs) under ambient vibration can be written as

$$M\left\{\ddot{x}(t)\right\} + C\left\{\dot{x}(t)\right\} + K\left\{x(t)\right\} = -M \cdot L \cdot \left\{\ddot{x}_s\left(t\right)\right\} \tag{5}$$

where M, C and K are the $n \times n$ mass, damping and stiffness matrices of the structure, respectively; $\{\ddot{x}(t)\}$, $\{\dot{x}(t)\}$ and $\{x(t)\}$ are respectively the nodal acceleration, velocity and displacement vectors of the structure; $\{\ddot{x}_s(t)\}$ is the applied ambient acceleration excitation at the supporting DOFs. L is the mapping vector of applied excitation at the associated DOFs of the structure. Rayleigh damping $C = a_1M + a_2K$ is assumed in this study, where a_1 and a_2 are the Rayleigh damping coefficients. The dynamic responses of the structure under ambient excitation can be computed from Eqn 5 with a time integration method, such as Newmark-β method (Newmark 1959).

When the system has zero initial conditions, the solution of Eqn 5 can be expressed in Duhamel integral as

$$\ddot{x}_p\left(t\right) = \int_{-\infty}^{t} \ddot{h}_p\left(t-\tau\right)\ddot{x}_s\left(\tau\right)d\tau \tag{6}$$

where $\ddot{x}_p(t)$ is the acceleration response at the sensor location p. $\ddot{h}_p(t)$ is the impulse response function at the pth DOF under the unit impulse ground motion.

The cross-correlation function $R_{pl}(t)$ of time-domain acceleration responses from sensor locations p and l can be expressed as follows (Bendat and Piersol 1980)

$$R_{pl}\left(\tau\right) = E\left\{\begin{aligned}&\int_{-\infty}^{t}\ddot{h}_p\left(t-\sigma_1\right)\ddot{x}_s\left(\sigma_1\right)\\&d\sigma_1\int_{-\infty}^{t+\tau}\ddot{h}_l\left(t+\tau-\sigma_2\right)\ddot{x}_s\left(\sigma_2\right)d\sigma_2\end{aligned}\right\} \tag{7}$$

where E denotes the expectation in statistics. Assuming that the structure is subject to a stationary random excitation, Eqn 7 can be further written as

$$R_{pl}(\tau) = \int_{-\infty}^{t}\int_{-\infty}^{t+\tau} \ddot{h}_p(t-\sigma_1)\ddot{h}_l(t+\tau-\sigma_2) \\ E\left(\ddot{x}_s(\sigma_1)\ddot{x}_s(\sigma_2)\right)d\sigma_1 d\sigma_2 \tag{8}$$

With the assumption that $\ddot{x}_s(t)$ is a white noise ambient excitation, the following relationship can be obtained

$$E\left(\ddot{x}_s(\sigma_1)\ddot{x}_s(\sigma_2)\right) = S\delta(\sigma_1 - \sigma_2) \tag{9}$$

where S is a constant which expresses the energy of the applied ambient vibration $\ddot{x}_s(t)$ when $\sigma_1 = \sigma_2$, and $\delta(t)$ is the Dirac delta function. Substituting Eqn 9 into Eqn 8 with $\int_{-\infty}^{+\infty} f(t)\delta(t)dt = f(0)$, we have

$$R_{pl}(\tau) = S\int_{0}^{\infty}\ddot{h}_p(t)\ddot{h}_l(t+\tau)dt \tag{10}$$

Eqn 10 indicates that the cross-correlation function between two time-domain responses resulting from an unknown white noise excitation has the form of the impulse response function of the structure. The cross-correlation function of two responses can also be obtained directly from the statistical computation as

$$R_{pl}(\tau) = E\left\{\ddot{x}_p(t)\ddot{x}_l(t+\tau)\right\} \tag{11}$$

3.2. Wavelet Packet Decomposition

Wavelet packets take linear combinations of the usual wavelet functions. A wavelet packet function is a function with three indices

$$\psi_{j,k}^{i}(t) = 2^{j/2}\psi^{i}\left(2^{j}t - k\right) \tag{12}$$

where integers i, j and k are the modulation, the scale and the translation parameter, respectively.

The wavelet functions ψ^i are obtained from the following recursive relationships

$$\begin{cases} \psi^{2i}(t) = \sqrt{2}\sum_{k=-\infty}^{\infty} h(k)\psi^{i}(2t-k) \\ \psi^{2i+1}(t) = \sqrt{2}\sum_{k=-\infty}^{\infty} g(k)\psi^{i}(2t-k) \end{cases} \tag{13}$$

where $h(k)$ and $g(k)$ are the quadrature mirror filters (Akansu and Haddad 1992) associated with the predefined scaling function and mother wavelet function. The first wavelet is the mother wavelet function with

$$\psi^{1}(t) = \psi(t) \tag{14}$$

The wavelet packet decomposition process is a recursive filter-decimation operation. Figure 1 shows a three-level wavelet packet decomposition of a time-domain signal $f(t)$. It can be seen that a complete decomposition at every level in both the low and high frequency ranges is achieved. The recursive relation between the jth and the $j + 1$ th level components is

$$\begin{cases} f_j^i(t) = f_{j+1}^{2i-1}(t) + f_{j+1}^{2i}(t) \\ f_{j+1}^{2i-1}(t) = Hf_j^i(t) \\ f_{j+1}^{2i}(t) = Gf_j^i(t) \end{cases} \tag{15}$$

where H and G are the filtering-decimation operators which are related to the discrete filters $h(k)$ and $g(k)$ by

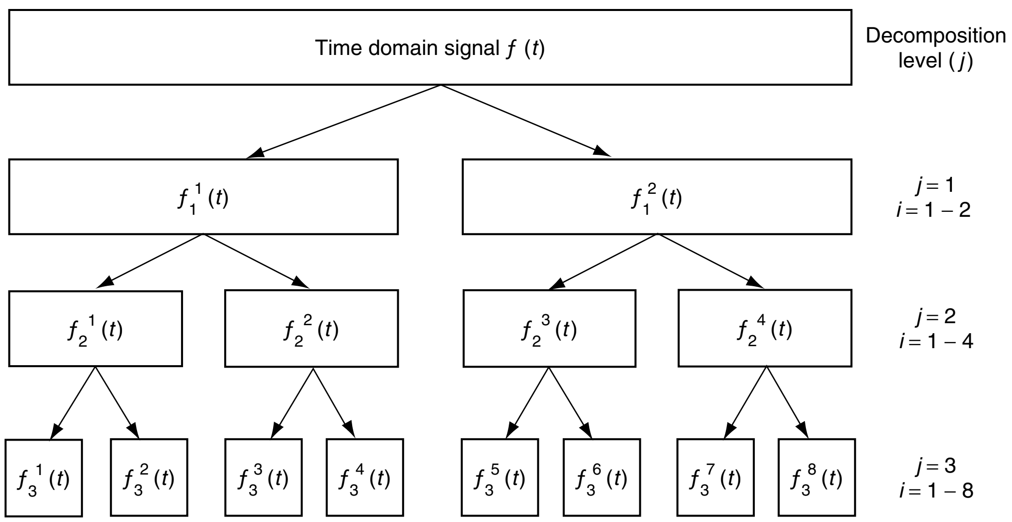

Figure 1. A three-level wavelet packet decomposition of a time-domain signal

$$\begin{cases} H\{\cdot\} = \sum_{k=-\infty}^{\infty} h(k-2t) \\ G\{\cdot\} = \sum_{k=-\infty}^{\infty} g(k-2t) \end{cases} \tag{16}$$

With jth level wavelet packet decomposition, the original signal $f(t)$ is expressed as

$$f(t) = \sum_{i=1}^{2^j} f_j^i(t) \tag{17}$$

in which, a wavelet packet component signal $f_j^i(t)$ can be expressed by a linear combination of wavelet packet functions $\psi_{j,k}^i(t)$ as follows

$$f_j^i(t) = \sum_{k=-\infty}^{\infty} c_{j,k}^i \psi_{j,k}^i(t) \tag{18}$$

where $c_{j,k}^i$ is the wavelet packet coefficient which is obtained from

$$c_{j,k}^i = \int_{-\infty}^{\infty} f(t)\psi_{j,k}^i(t)\,dt \tag{19}$$

Yen and Lin (2000) investigated the feasibility of applying the wavelet packet transform to the classification of vibration signals, and wavelet packet energy has been explored for damage assessment (Sun and Chang 2004; Han *et al*. 2005). The definition of wavelet packet energy is

$$E_f = \sum_{i=1}^{2^j} E_{f_j^i} \tag{20}$$

where E_f is the total wavelet packet energy of a signal record $f(t)$; $E_{f_j^i}$ is the ith wavelet packet component energy at the jth level of decomposition and is obtained as the energy stored in the component signal $f_j^i(t)$

$$E_{f_j^i} = \int_{-\infty}^{\infty} f_j^i(t)^2\,dt \tag{21}$$

Eqn 20 shows that the total wavelet packet energy of a signal is a summation of all the wavelet packet component energies in different frequency bandwidths and Eqn 2 denotes the wavelet packet energy in a specific frequency bandwidth which is determined by the number of wavelet packet and the level of wavelet packet decomposition.

3.3. Damage Detection with Wavelet Packet Energy of Cross-Correlation Function

The cross-correlation function between slab response and the corresponding girder response can be derived theoretically from Eqn 10:

$$\frac{R_{sg}(\tau)}{S} = \int_0^{\infty} \ddot{h}_s(t)\ddot{h}_g(t+\tau)\,dt \tag{22}$$

where, $\ddot{h}_s(t)$ and $\ddot{h}_g(t+\tau)$ denote the impulse response functions at the slab and corresponding girder sensor locations and $R_{sg}(\tau)$ is the cross-correlation function between slab and girder responses. It should be noticed that $R_{sg}(\tau)/S$ is a function of the impulse response functions at sth and gth DOFs only, in which S expresses the energy magnitude of the ambient vibration. With the wavelet packet decomposition of cross-correlation function $R_{sg}(\tau)$ performed, the wavelet packet coefficients of each component can be obtained and then the wavelet packet component energy $E_{f_j^i}$ and the total wavelet packet energy E_f are computed. Since E_f is determined from the ambient vibration energy level, the percentage of a specific wavelet packet component energy to the total wavelet packet energy $E_{f_j^i}/E_f$ is also a function of impulse response functions at sth and gth DOFs and therefore is a function of system parameters.

The damage detection will be conducted based on the change of the energy percentage of wavelet packet components in selected frequency bandwidths:

$$DI = \frac{|P_d - P_{ud}|}{P_{ud}} \tag{23}$$

where DI is the damage index, P_d and P_{ud} are the percentages of wavelet packet components energy in the selected frequency bandwidths to the total wavelet packet energy from the damaged and undamaged structures, respectively. They may include a wavelet packet with a specific frequency range or several wavelet packets with selected frequency ranges.

3.4. Establishment of a Threshold Value for Damage Detection

When n damage indices at different sensor locations are obtained from Eqn 23, the mean value and standard deviation of these damage indices can be computed and expressed as μ and σ. The one-side upper confidence limit for the damage index can be defined as (Han *et al*. 2005):

$$UL = \mu + Z_\alpha \times \frac{\sigma}{\sqrt{n}} \tag{24}$$

where Z_α is the value of a standard norm distribution with zero mean and unit standard deviation such that the cumulative probability is 100 × (1–α)%. The upper confidence limit UL is considered as a threshold value to indicate possible abnormalities in the structure. The definition of this threshold value is based on the statistical properties of the calculated damage indices from measured ambient responses. Damage index values which are larger than the threshold value indicate the locations of possible damages. Others smaller than the threshold value are the undamaged locations. This statistical definition of a threshold value is also adopted in Ref. (Ren *et al*. 2008). With consideration of the threshold value, a new damage indicator ($DI - UL$) is used in this study to identify damage, in which DI is the damage index obtained from Eqn 23. It should be noticed that the undamaged locations are determined when the damage index value DI is less than the threshold value. To highlight the detected damage locations, the values of ($DI - UL$) on undamaged locations are taken as zeros and the positive values of ($DI - UL$) on damaged locations will be shown.

3. NUMERICAL STUDIES

Numerical studies on a simply-supported slab-on-girder bridge are conducted to illustrate the accuracy and efficiency of the proposed approach for damage detection of shear connectors with ambient vibration measurements. Figure 2 shows the plan view, cross section of the structure and details of a shear connector. The concrete slab is supported on two steel I-type girders, and shear connectors are used to link the slab and girders together. Two ends of steel girders are simply supported. Each girder has sixteen shear connectors with equal space and there are thirty-two shear connectors in total in the structure. They are denoted as SC1~SC32 in Figure 2(a). The cross-section of the structure is shown in Figure 2(b). To be consistent as the laboratory tests that will be described later, the shear connector is simulated as a metric bolt screwing into a metal nut, as shown in Figure 2(c). The failure of bolts will cause the shear slippage between the slab and girder and reduce the

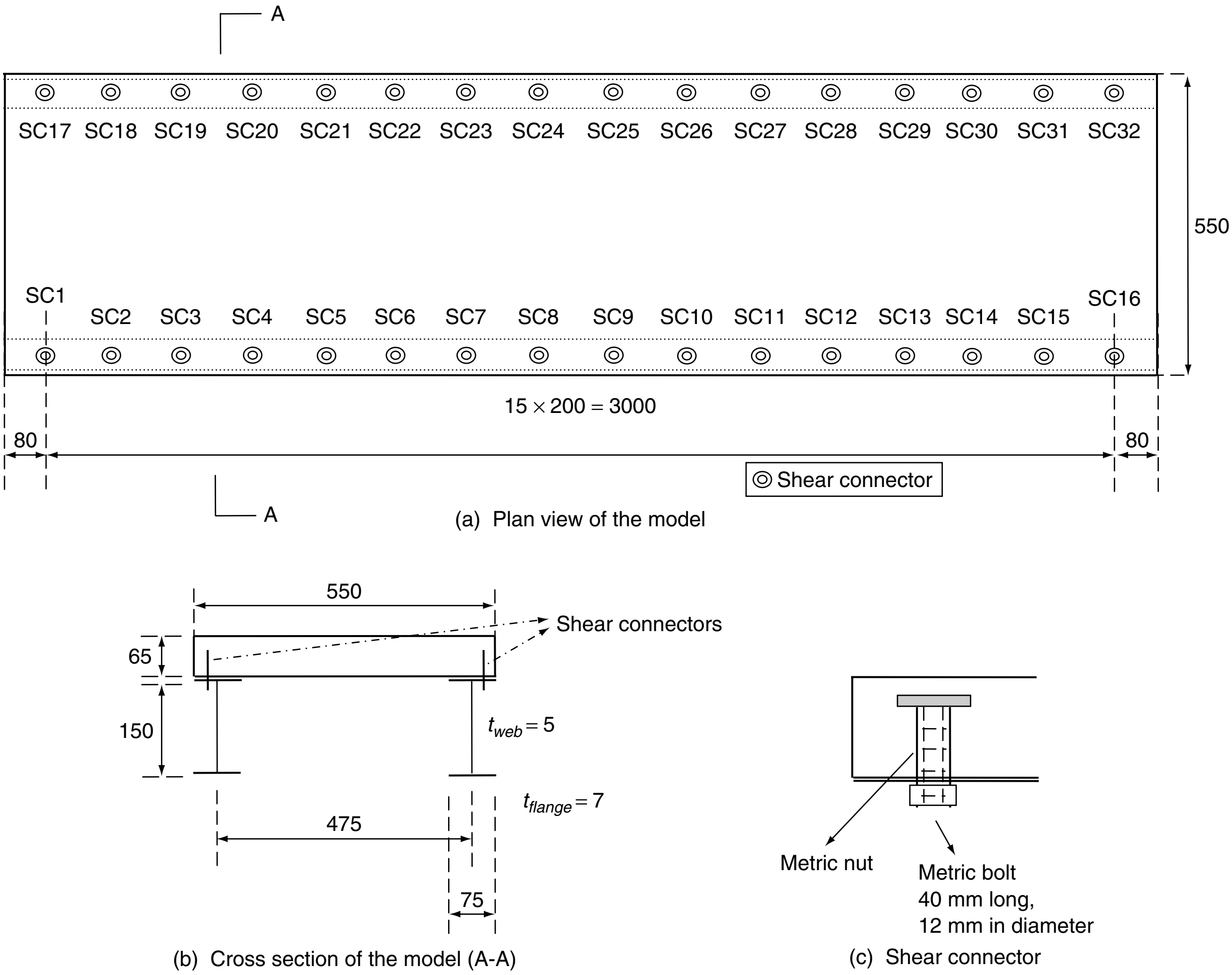

Figure 2. Dimensions and shear connector details of the slab-on-girder structure (unit: mm)

load-carrying capacity of composite bridges. The bolt is fully unscrewed from the metal nut to simulate the failure of shear link in this study. The identification with different damage servilities of shear connectors is not conducted in this paper.

3.1. Finite Element Model and Sensor Placement Configuration

Slab and steel girders are modeled with shell elements, and shear connectors are modeled with beam elements (Xia *et al*. 2008) that link the slab and girders. The axial stiffness and shear stiffness of a shear connector are obtained by the formulas from an existing study (Chiewanichakorn *et al*. 2004) and are 2.64×10^3 N/m and 8.64×10^5 N/m, respectively. The finite element model of the slab-on-girder structure consists of 695 nodes, 600 shell elements and 32 beam elements. Each node has six DOFs and the system has 4170 DOFs in total. The Young's modulus and mass density of slab concrete are 3.18×10^4 MPa and 2500 kg/m^3, respectively. The Young's modulus and mass density of steel girder are 2×10^5 and 8092 kg/m^3, respectively. The first three natural frequencies in the vertical direction are 35.9 Hz, 113.96 Hz and 144.96 Hz, respectively. Rayleigh damping is assumed and the damping ratios for the first two modes are taken as $\xi = 0.012$.

Figure 3 shows the locations of accelerometers placed on the slab, denoted as "SA1-SA8" and "SB1-SB8", and those underneath the girders, denoted as "GA1-GA8" and "GB1-GB8", for measurement of the acceleration responses under ambient tests. A reference accelerometer measurement is used to extract the mode shape, as shown in Figure 3. 100000 data points of measured responses with a sampling rate of 1000 Hz are used to compute the cross-correlation function with Eqn 11. Shear forces of a simply-supported structure at the two support locations are generally larger than those at other places. Therefore damages of shear connectors are normally presented near the supports. Two damage scenarios are assumed, as shown in Table 1.

The ambient excitation is assumed as a Gaussian noise and applied in the vertical direction of the structural model

$$\ddot{x}_s(t) = S\Phi(t) \tag{25}$$

where $\Phi(t)$ is a standard normal distribution. As the ambient vibration level in each test is different, three

Table 1. Damage scenarios in numerical study

Damage scenario	Shear connectors removed
Scenario 1	SC1, SC2, SC15, SC16, SC17, SC18, SC31 and SC32
Scenario 2	SC1, SC2, SC15 and SC16

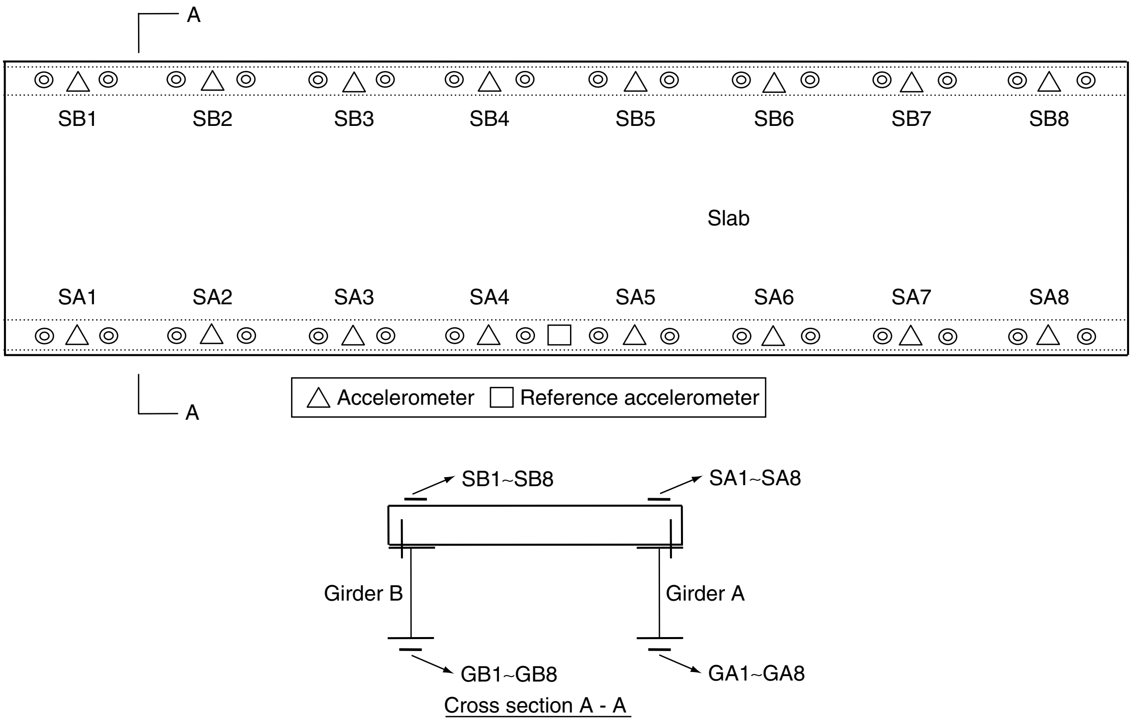

Figure 3. Sensor locations on the slab and underneath the girders

ambient excitation levels are assumed in this study to numerically validate that the proposed dynamic assessment approach is valid for different ambient excitation energy magnitudes. The adoptions of S value for undamaged case, damage Scenario 1 and damage Scenario 2 are 0.01, 0.03 and 0.02, respectively. Figure 4 shows the simulated ambient excitation acceleration records for the undamaged and damaged states. It should be noticed that these simulated excitations are used to excite the structure and not required in the damage identification.

To simulate the effect of measurement noise, a normally distributed random noise with zero mean and unit standard deviation is added to the calculated dynamic response as

$$\ddot{x}_n = \ddot{x}_{cal} + E_p N_{oise} std(\ddot{x}_{cal}) \quad (26)$$

where $\ddot{x}_n$ and $\ddot{x}_{cal}$ are the simulated response with noise effect and the original calculated response, respectively; E_p is the noise level and equals to 0.05 if 5% noise is included in the response; N_{oise} is a standard normal distribution vector with zero mean and unit standard deviation and $std(\ddot{x}_{cal})$ denotes the standard deviation of the original calculated response. It may be noted that this is one of several approaches to simulate the noise effect in the measured responses. Two noise levels, namely 5% and 10%, are included in the simulated "measured" acceleration responses.

3.2. Damage Detection Results with Identified Modal Information

The modal information, such as frequencies and mode shapes, is identified based on the Frequency Domain Decomposition method (Brincker *et al.* 2000). Natural frequencies of the identified two modes of the structure in the undamaged and damaged states are shown in Table 2. These significant changes in frequencies are observed because the shear connectors at the two support locations are removed and this structure has no diaphragms at the two ends. This observation is consistent with a reported study. It has also been

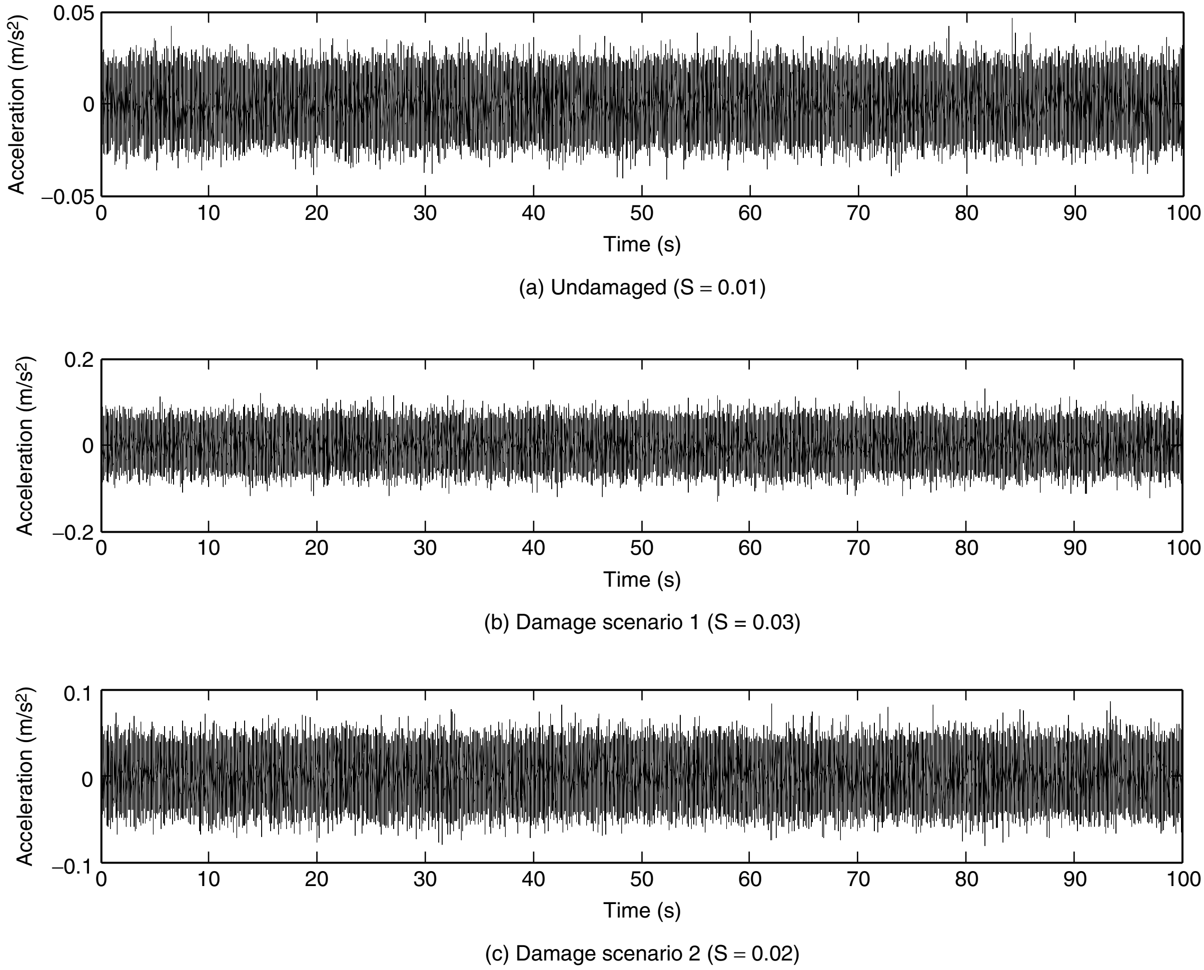

Figure 4. Simulated ambient excitation acceleration records for the undamaged and damaged states

Table 2. Identified frequencies of the undamaged and damaged structures in numerical study

Mode	Undamaged (Hz)	Scenario 1 (Hz)	Change (%)	Scenario 2 (Hz)	Change (%)
1	35.89	32.55	9.31	33.91	5.52
2	110.2	93.58	15.08	104.83	4.87

reported (Dilena and Morassi 2003; Morassi and Rocchetto 2003) that significant frequency variations, even more than 20% in some modes, are found in flexural vibration modes of composite structures due to the damage of shear connectors, and the detection with frequency shifts may give false identification results because damage in symmetric areas will produce identical changes in natural frequencies.

Modal Assurance Criterion (MAC) values of these two identified mode shapes at the slab sensor locations of two damage scenarios are shown in Table 3. The MAC value for the first mode of two damage states is 0.96 and is just greater than 0.6 for the second mode indicating clearly the existence of the damage. For the particular cases considered in this study, the second mode is more significantly affected than the first mode because shear link damage results in the deck and girder to bend independently with shear slip along the interface. The second mode shape has larger curvature than the first mode shape, indicating more intensive relative displacement along the deck and girder interface. Therefore the second mode is more affected by shear link damage than the first mode. Figure 5 shows the identified mode shapes of the undamaged structure from simulated measured responses without noise. The identified mode shapes in the undamaged and damaged states are used to compute the COMAC values. COMAC is similar to MAC, but is spatially referenced to each sensor location. A lower COMAC value indicates the area of discrepancy between the undamaged and damaged mode shapes and may locate the damage. Figures 6(a) and 6(b) show the COMAC values in both girders for damage Scenarios 1 and 2, respectively. It can be seen from Figure 6(a) that lower COMAC values at sensor locations SA1, SA8, SB1 and SB8 are observed. In Scenario 2, lower COMAC values

Table 3. MAC values of the damaged structure in numerical study

Mode	Damaged scenario 1	Damaged scenario 2
1	0.96	0.96
2	0.61	0.63

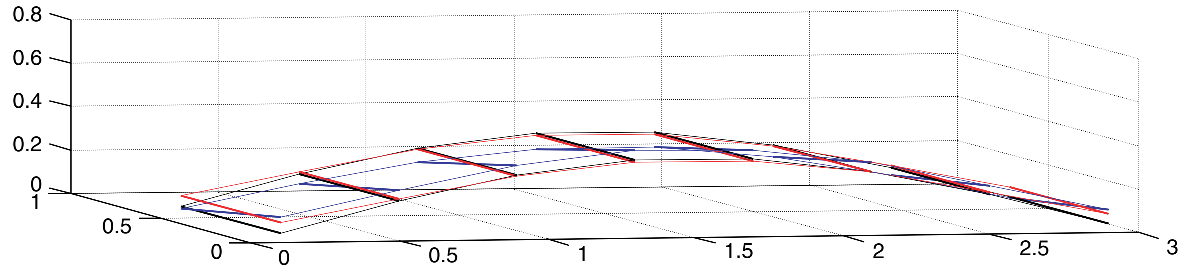

(a) First mode

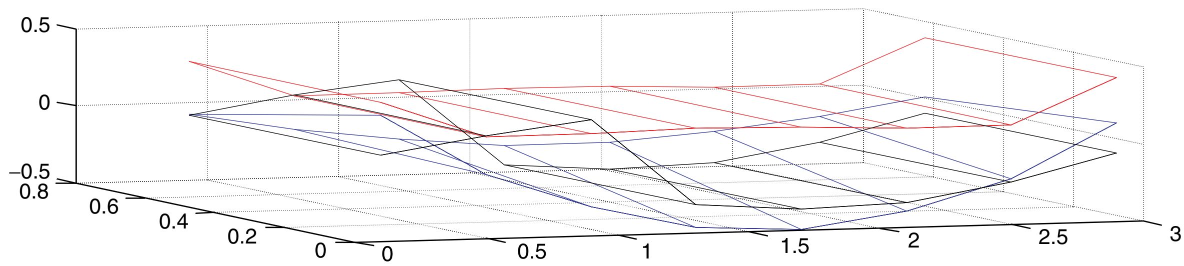

(b) Second mode

Figure 5. Identified mode shapes from ambient measurements without noise in numerical study (Dark line: Undamaged state, Red line: Damage Scenario 1, Blue line: Damage Scenario 2)

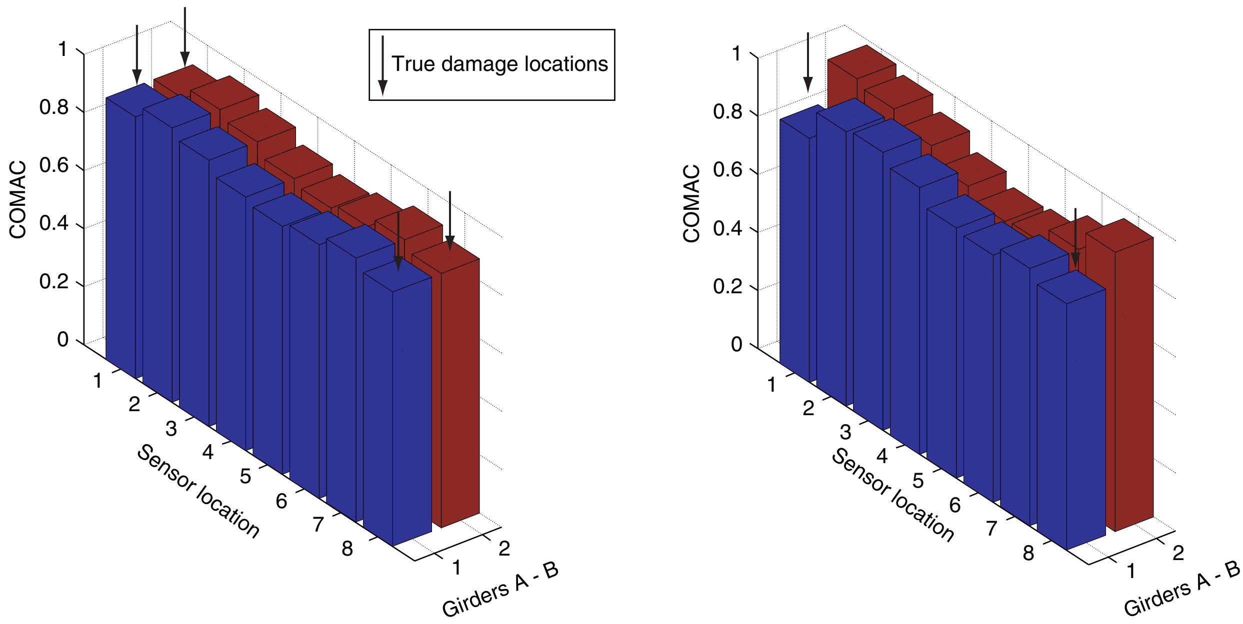

(a) Damage scenario 1

(b) Damage scenario 2

Figure 6. Damage detection results with COMAC in numerical study

at sensor locations SA1 and SA8 are found from Figure 6(b). However, it can be seen that many false identifications present in the detection results of both scenarios especially in the central span area even that the MAC value clearly indicates the existence of damage as shown in Table 3. The detection results with COMAC using identified mode shapes from measured responses including noise effect would be much worse.

Figure 7 shows the identification results with changes in flexibility for Scenarios 1 and 2. The damages of shear connectors at support locations in Scenario 1 can be identified, while there are some false identifications in the center span probably because the response in the mid-span is the largest and the difference in the mode shapes at the center span sensor locations is also picked up as damages. The damages of shear connectors at

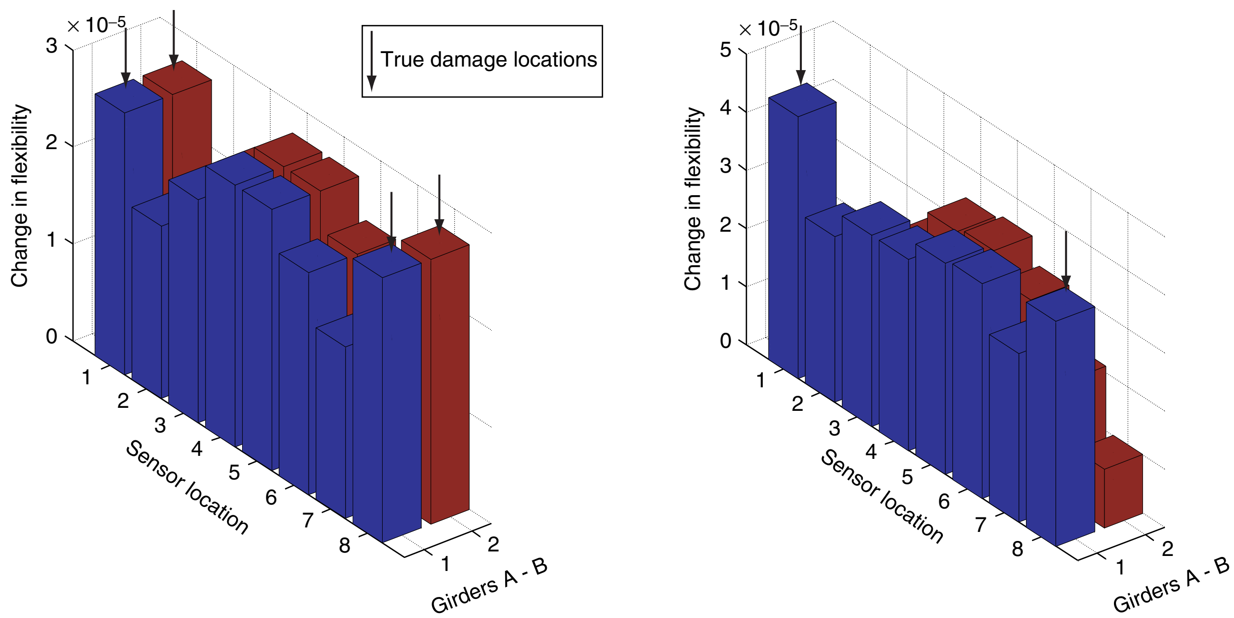

(a) Damage scenario 1

(b) Damage scenario 2

Figure 7. Damage detection results with changes in flexibility

sensor locations SA1 and SA8 in Scenario 2 are identified correctly with the changes in the flexibility. Similarly, the damage index values in the center are also relatively high and are false identifications.

3.3. Damage Detection Results with Wavelet Packet Energy of Cross-Correlation Functions

Measured acceleration responses from the structure in the undamaged and damaged states under ambient excitations are obtained to compute the cross-correlation function between slab and girder responses with Eqn 11. Wavelet packet decomposition of the calculated cross-correlation function is performed and the wavelet packet energy of each specific component can be obtained. It has been studied and reported (Sun and Chang 2004; Han *et al*. 2005) that wavelet packet energy of the components with the lower frequency bandwidths are more sensitive than the original signal and the energy with high frequency bandwidths are even more sensitive. However, the wavelet packet energy of the high frequency range is relatively small and thus more vulnerable to the influence of measurement noise that makes the packet energy in high frequency range not reliable for damage assessment. In this regard, it may be more reliable and stable to use the wavelet packets with lower frequency bandwidths for damage detection. In the simulation study, a three-level wavelet packet decomposition is performed and the frequency bandwidths of all the wavelet packets are shown in Table 4. It can be noticed that the identified two modes lie in the first and second wavelet packets respectively and then the energy percentage of these two wavelet packets to the total wavelet packet energy is used to compute the damage index with Eqn 23 as this could be a more reliable and robust option. α is set to be 0.05 in Eqn 24 to obtain the upper confidence limit and then compute the damage indicator ($DI–UL$) with consideration of this threshold value. Figure 8 shows the damage detection results of two damage scenarios from measured responses without noise effect. Identified results of Scenario 1 for Girders A and B are shown in Figure 8(a). It can be clearly seen that high damage indices at sensor locations No. 1 and No. 8 in both girders are observed indicating the simulated damage locations are identified correctly. Figure 8(b) shows the detection results of Scenario 2. Damage index values at sensor location No. 1 and No. 8 in Girder A are around

Table 4. Frequency bandwidth of wavelet packets in numerical study

Wavelet packet number	Frequency bandwidth (Hz)	Identified mode
$f_3^1(t)$	0 - 62.5	1
$f_3^2(t)$	62.5 - 125	2
$f_3^3(t)$	125 - 187.5	
$f_3^4(t)$	187.5 - 250	
$f_3^5(t)$	250 - 312.5	
$f_3^6(t)$	312.5 - 375	
$f_3^7(t)$	375 - 437.5	
$f_3^8(t)$	437.5 - 500	

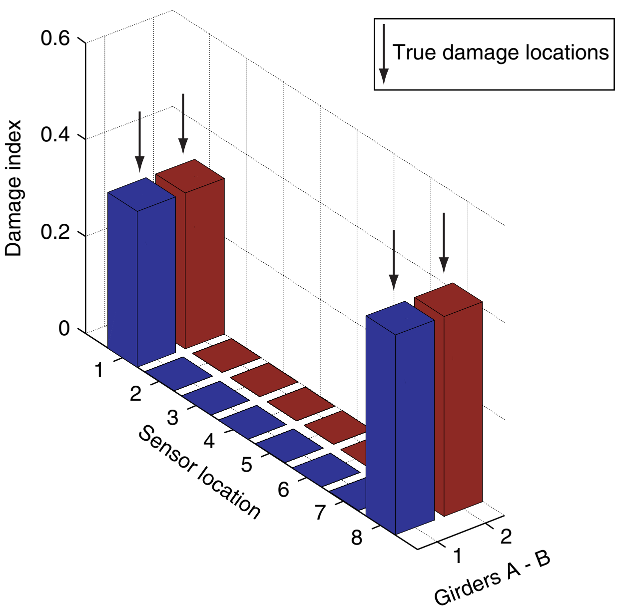

(a) Damage scenario 1

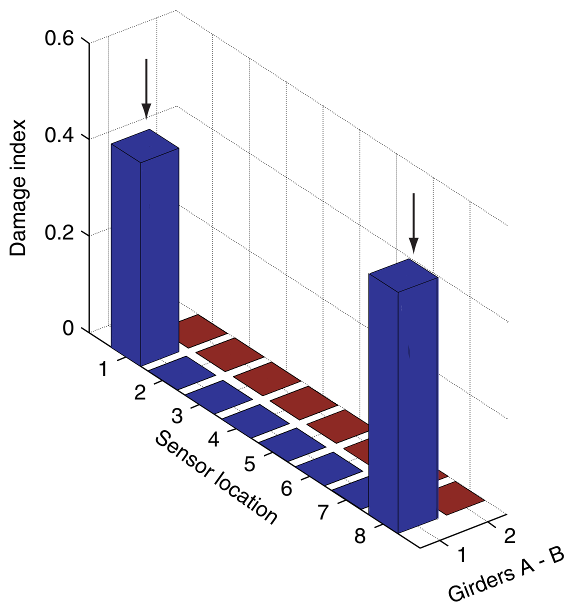

(b) Damage scenario 2

Figure 8. Damage detection results from measured responses without noise effect

0.4, indicating the existence of shear connector damages in these sensor locations. The identified locations in two scenarios match well with the introduced damage locations with no false identification.

Figure 9 shows the detection results from the simulated responses with 5% noise and 10% noise. The introduced damage locations of two scenarios can be detected accurately with two noise levels considered in the study. It should be noticed that the damage index values identified from measured responses with two noise levels are close to those in the detection results without noise. The well robustness and performance of the proposed approach for damage detection of shear connectors under ambient excitation from noisy measurements are demonstrated.

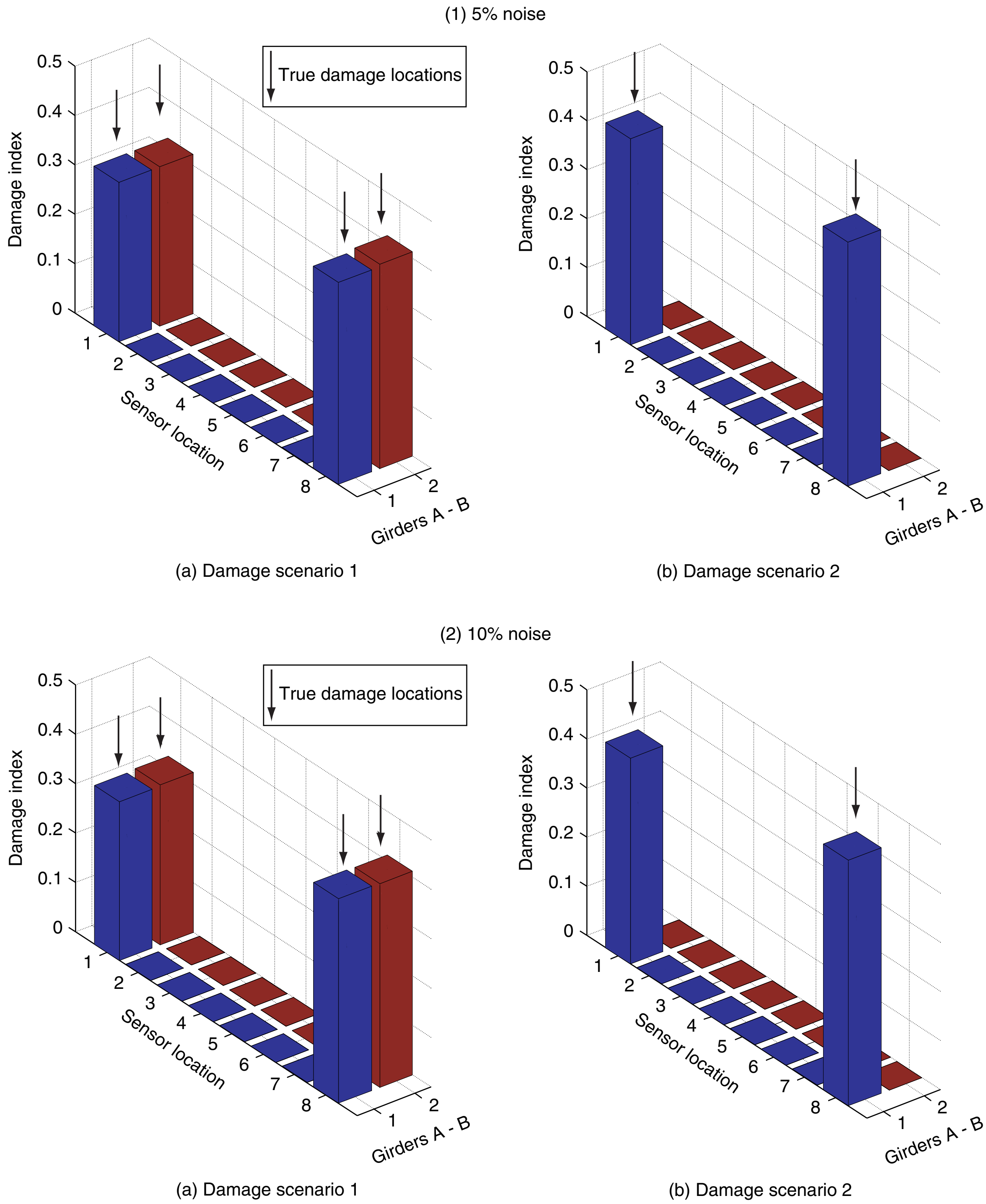

Figure 9. Damage detection results from measured responses with noise effect

It is numerically validated that the introduced damages of shear connectors in both scenarios are identified accurately with no false identification even the vibration signals are smeared with a high noise level. It should be noted that damage locations of shear connectors are not likely to be detected with visual inspections because they are buried inside the structures, and difficult to be confidently identified with the modal information based parameters such as COMAC and changes in flexibility because many false identifications may present.

4. EXPERIMENTAL VERFICATION

4.1. Experimental Setup

Experimental studies on a composite bridge are conducted to validate the proposed damage detection approach. A slab-on-girder structure is fabricated and tested in the lab, and the measured responses under environmental ambient vibration are used for the damage detection. The performance of the proposed approach for the damage identification of shear connectors with experimental testing data is investigated.

The testing model was constructed with a concrete slab supported on two steel girders. Sixteen shear connectors were mounted with equal space in each girder to link the slab and steel girder together. It was located on two steel frames which were fixed on the strong ground as shown in Figure 10. The design of shear connectors considers the ability not only to simulate failure of specific shear links, but also to reset-up them to the undamaged state. Therefore, a metric bolt screwing into a metric nut connecting the slab and girder was used as the shear connector. The metric nuts were welded onto the reinforcement bar in the slab before pouring. Design and setup of shear connectors can be seen in Figure 11. If all the bolts are screwed into their nuts, the structure condition corresponds to the undamaged state. The damage of shear connectors is introduced into the structure by fully unscrewing several specific metric bolts

Figure 10. Experimental setup of the slab-on-girder structure

(a) Metric bolt and nut

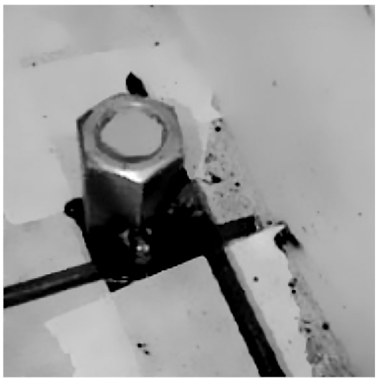

(b) Bolt screwed into the nut

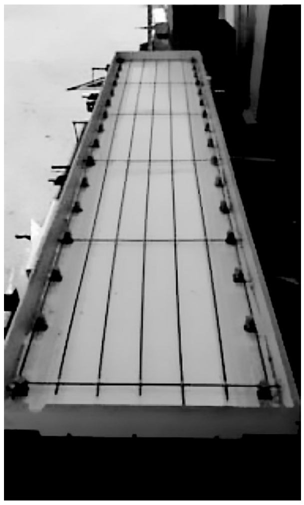

(c) Plan view of shear connectors

(d) Shear connector in the structure

Figure 11. Design of shear connectors

to simulate the failure of shear link. The dimensions of the laboratory model are the same as those of the model in the numerical study. The proposed damage detection approach for shear connectors is non-model based as the finite element model of the structure is not required. Therefore the dimensions, boundary conditions of the model and material properties of the slab, girder and shear connectors are not introduced because they are not required for damage identification. In the paper, both numerical simulations and experimental tests are conducted to demonstrate the validity of the method. The data from them are treated independently to identify the damage. There is no need to the model updating to service as the baseline finite element model.

Nine Kistler 8330A3 accelerometers were used in the laboratory ambient tests to collect the acceleration responses of the structure. A sixteen-channel conditioner and data acquisition system was employed to record acceleration signals. The measuring sampling frequency was set as 2000 Hz. Figure 12 shows the numbering of shear connectors and sensor locations defined in the tests. One reference sensor is used to extract the mode shape from repeated ambient tests with different sensor layouts. Four tests are conducted to measure all the responses on the slab and underneath the girders under ambient vibrations, for example, with one sensor on the reference location and the first set with eight sensors to measure the responses at SA1-SA4 and GA1-GA4, the second set at SA5-SA8 and GA5-GA8, the third set at SB1-SB4 and GB1-GB4 and the final set at SB5-SB8 and GB5-GB8. The same damage scenarios defined in numerical studies are used here. 200000 data points with a sampling rate of 2000 Hz are recorded from each sensor.

4.2. Damage Detection Results with Identified Modal Information

The identified frequencies of the undamaged and damaged structures are listed in Table 5. MAC values at the slab sensor locations of two damage states are shown in Table 6. It can be seen from Tables 5 and 6

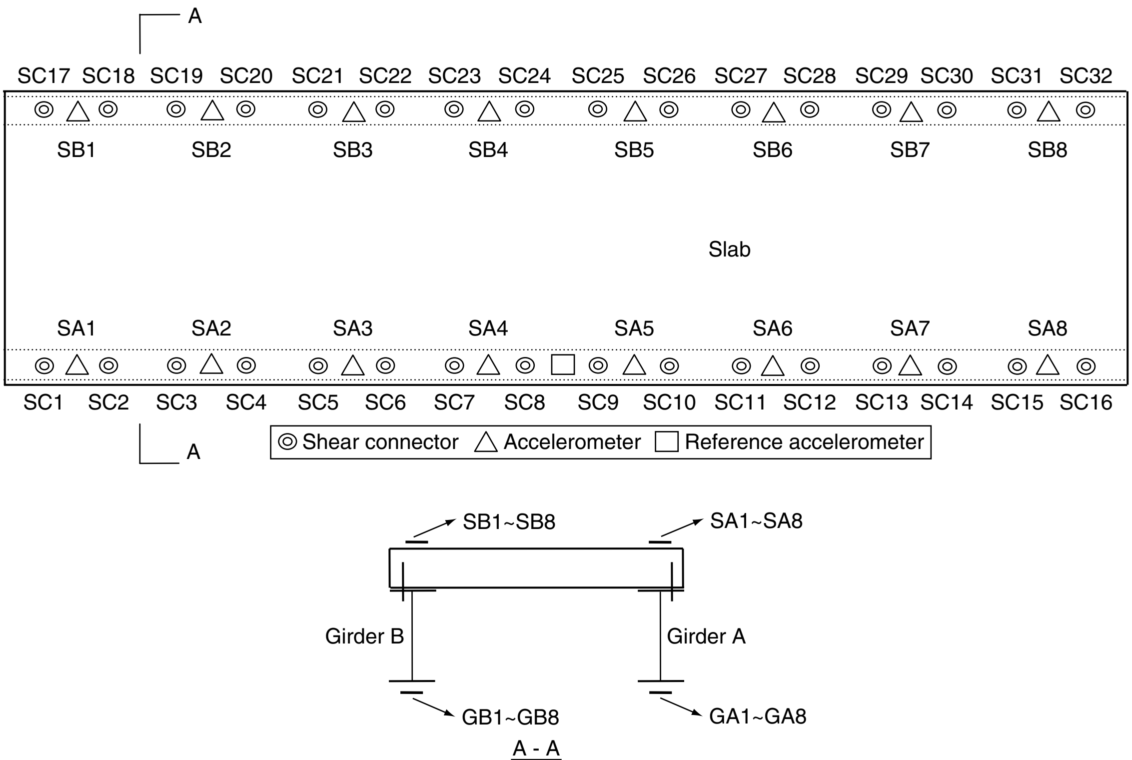

Figure 12. Experimental sensor placement

Table 5. Identified frequencies of the undamaged and damaged structures in experimental study

Mode	Undamaged (Hz)	Damaged scenario 1 (Hz)	Error (%)	Damaged scenario 2 (Hz)	Error (%)
1	41.42	36.15	12.7	38	8.26
2	113.2	86.95	23.19	97.11	14.2

Table 6. MAC values of the damaged structure in experimental study

Mode	Damaged scenario 1	Damaged scenario 2
1	0.984	0.974
2	0.853	0.825

that significant changes of the identified frequencies are observed in two damage scenarios. This observation is consistent with that in the numerical study. The changes of MAC values, especially for the second mode, indicate clearly the occurrence of damage in these two scenarios. Figure 13 shows the corresponding identified mode shapes of the undamaged structure. The identified mode shapes in the undamaged and damaged states are used to compute the COMAC value to detect the damage of shear connectors. Figures 14(a) and 14(b) show the damage detection results with COMAC for Scenarios 1 and 2, respectively. The detection with COMAC may not give good results in both scenarios. False identification exists in the central span because a low signal to noise ratio exists in the measured responses with a low ambient vibration level. Figure 15 shows the damage detection results with changes in flexibility. It can be seen that the introduced damages are identified while with several false identifications, such as, sensor locations SA7, SB2, SB3 in Scenario 1, Sensor locations SA7, SB1, SB2 and SB3 in Scenario 2.

4.3. Damage Detection Results with Wavelet Packet Energy of Cross-Correlation Functions

Ambient tests were conducted in both the undamaged and damaged states, and acceleration response data on the slab and girders were measured for damage identification. Cross-correlation function between slab and girder responses is obtained for a four-level wavelet packet decomposition. Table 7 shows the frequency bandwidth of each wavelet packet, and it can be seen that the identified first and second frequencies are included in the first and second wavelet packets, respectively. Therefore the energy percentage of the first and second wavelet packets is used to compute the damage index with Eqn 23. Since more uncertainties may exist in the experimental testing and the ambient vibration level in the laboratory is quite low making the structural responses small, α is set as 0.1 such that the cumulative probability of the upper confidence limit is 90% to provide a robust tolerance to detect the damage.

Figure 16 shows the cross-correlation functions between sensor locations SA4 and GA4 in the undamaged and damaged states. The magnitudes and shapes of those cross-correlation functions are different because the ambient excitations and energy levels are different in the tests for undamaged and damaged states. The wavelet packet analysis is then performed to extract the stable damage feature and calculate the damage index. Figures 17(a) and 17(b) show the identified results of damage Scenarios 1 and 2, respectively. It can

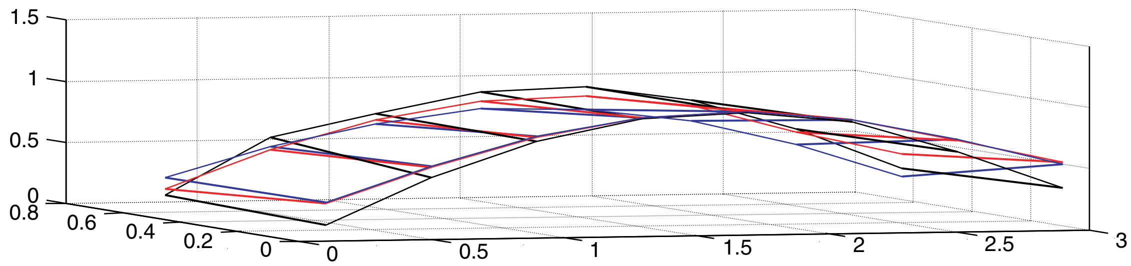

(a) First mode

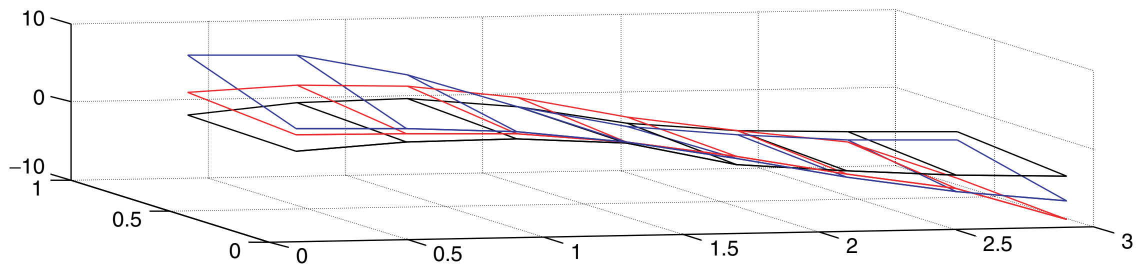

(b) Second mode

Figure 13. Identified mode shapes of the undamaged structure in experimental study

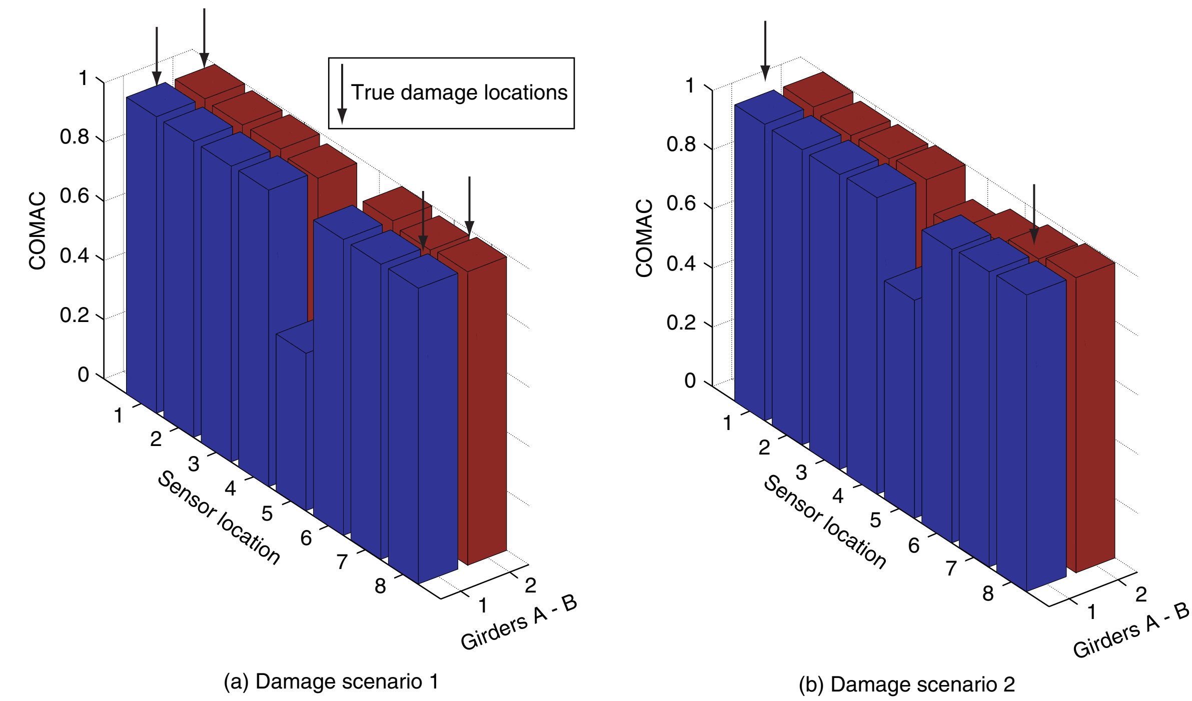

Figure 14. Damage detection results with COMAC in experimental study

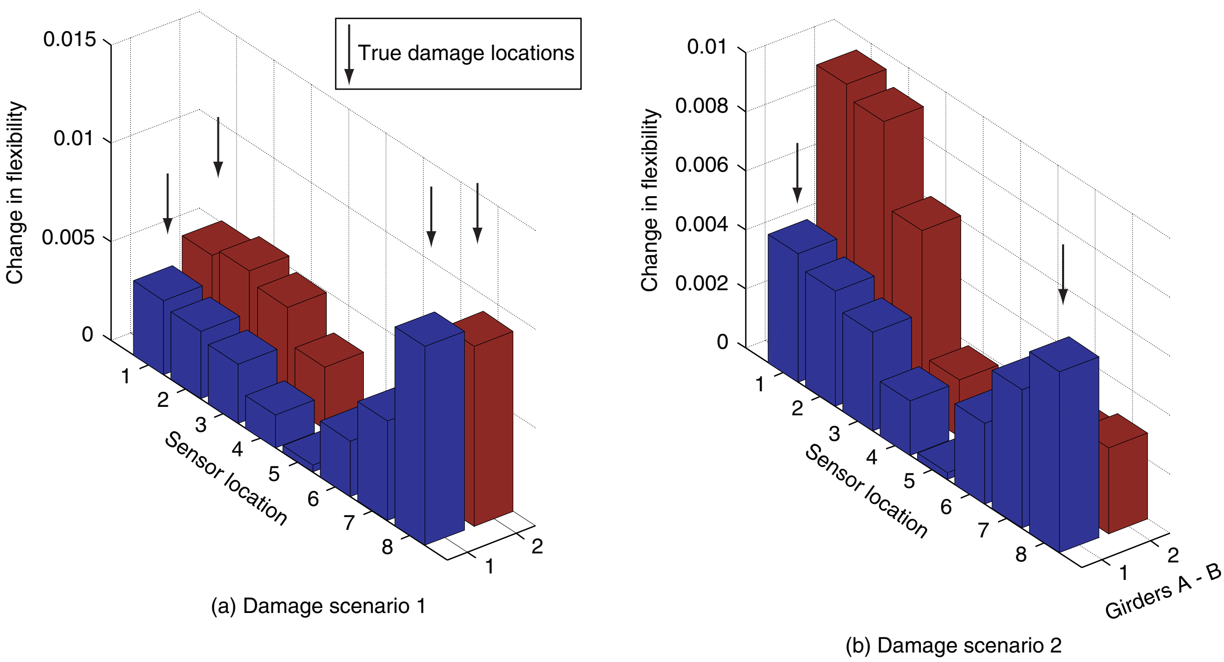

Figure 15. Damage detection results with changes in flexibility

be found that high damage index values at the sensor locations No.1 and No.8 in two girders are obtained, indicating that the damages of shear connectors are presented in these areas in damage Scenario 1. This observation illustrates that the introduced damage of shear connectors are identified correctly. It should be noticed that the damage indices at the sensor location No.1 in two girders are generally larger than those at the sensor location No.8 although the damage severities at these two locations are the same. One possible reason for this difference is the possible different frictions between the steel girders and concrete slab. Although the two steel girders used in the structure model are the same, the surface conditions of the concrete slab at the

Table 7. Frequency bandwidth of wavelet packets in experimental study

Wavelet packet number	Frequency bandwidth (Hz)	Identified mode
$f_4^1(t)$	0 - 62.5	1
$f_4^2(t)$	62.5 - 125	2
$f_4^3(t)$	125 - 187.5	
$f_4^4(t)$	187.5 - 250	
$f_4^5(t)$	250 - 312.5	
$f_4^6(t)$	312.5 - 375	
$f_4^7(t)$	375 - 437.5	
$f_4^8(t)$	437.5 - 500	
$f_4^9(t)$	500 - 562.5	
$f_4^{10}(t)$	562.5 - 625	
$f_4^{11}(t)$	625 - 687.5	
$f_4^{12}(t)$	687.5 - 750	
$f_4^{13}(t)$	750 - 812.5	
$f_4^{14}(t)$	812.5 - 875	
$f_4^{15}(t)$	875 - 937.5	
$f_4^{16}(t)$	937.5 - 1000	

two end locations might be different owing to construction quality control, which results in different frictions between steel girders and concrete slab and hence affects the calculated damage indices at the two locations. Moreover, this observation also indicates that the absolute damage index value may not be used to quantify the damage. This limitation is the same as other non-model based methods, i.e., they can locate the damage but very difficult to quantify the damage. Shear connectors SC1 and SC2 near the sensor location SA1, and SC15 and SC16 near the sensor location SA8, were removed in Scenario 2. It can be found that these two introduced damage locations are identified accurately. A very small false identification appears in sensor location No.8 in Girder B as this area is close to the true damage location at SA8. It is also found that the damage index in Girder A at the sensor location No.8 is smaller than that at the sensor location No. 1 with the same observation and possible reason explained above.

Experimental studies demonstrated that the proposed dynamic assessment approach based on wavelet packet energy of cross-correlation functions from ambient vibration measured accelerations can identify the damage locations of shear connectors accurately and efficiently. The robustness and performance of the proposed approach is good. Only a few false identifications might occur, the proposed method can be used effectively to identify possible shear connector damages that cannot be reliably detected by routine visual inspections.

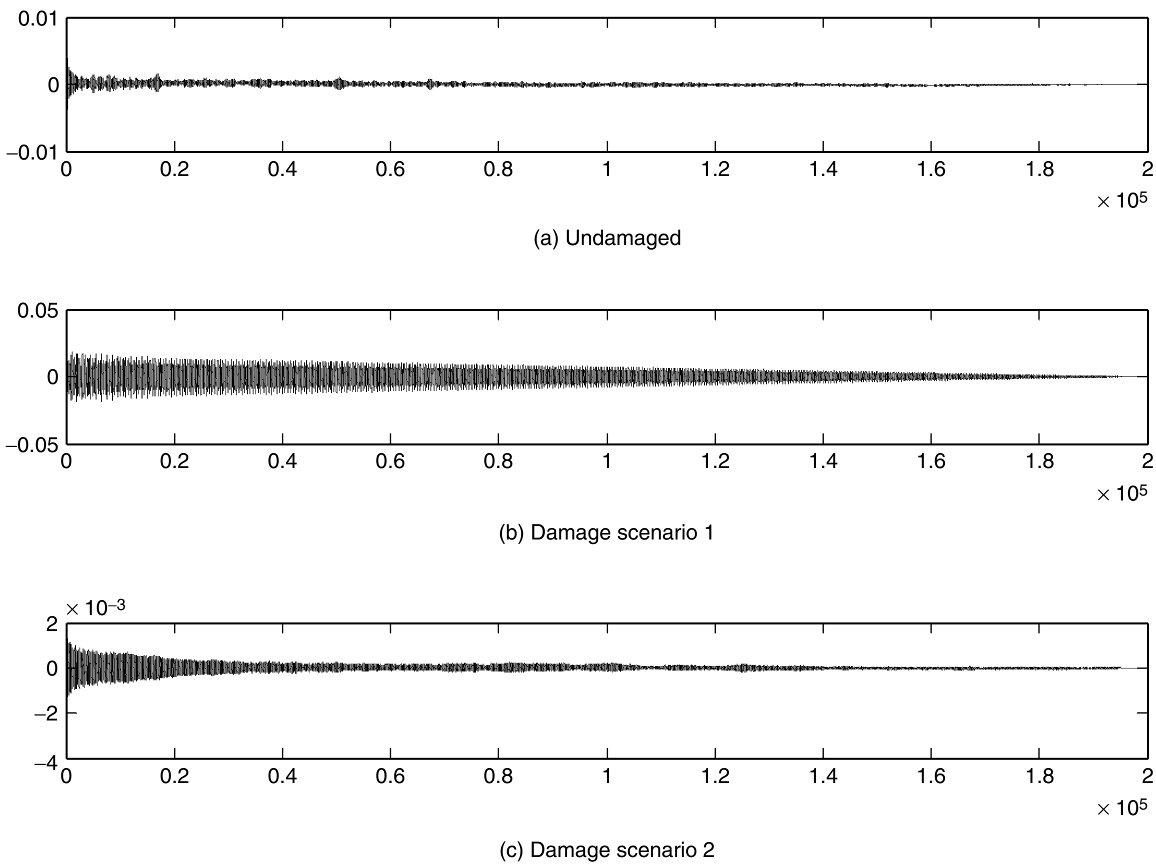

Figure 16. Cross-correlation functions between sensor locations SA4 and GA4

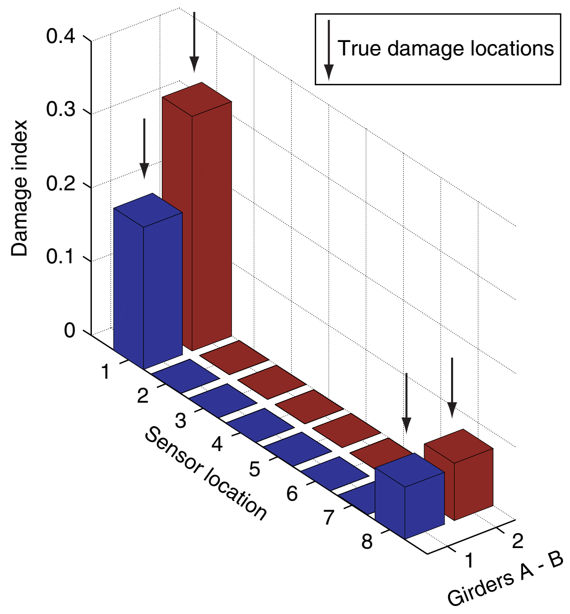

(a) Damage scenario 1

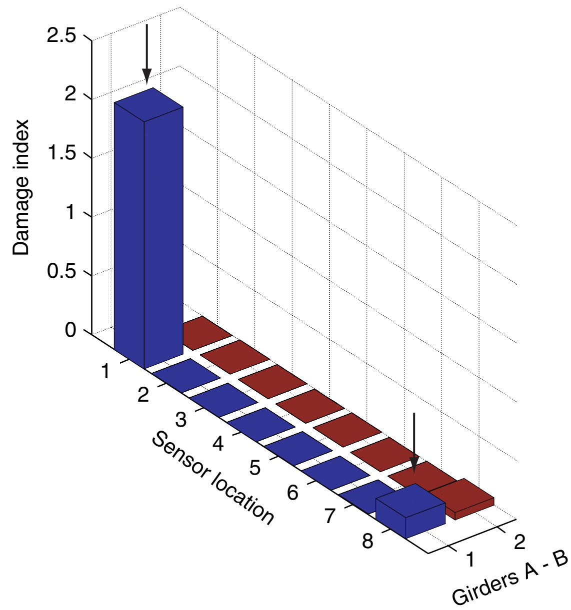

(b) Damage scenario 2

Figure 17. Damage detection results with measured responses in experimental study

5. DISCUSSIONS

In real situations, bridges subject to loads, such as mainly traffic loading and/or pedestrian loading for short and medium span bridges. Therefore the shear forces will exist at the interface of slab and girders in composite bridges. In this case, damages of shear connectors will introduce a significant shear slippage in the structure and induce a significant difference in the responses on the slab and girder. Four concrete mass blocks, weighted around 0.6ton, are placed on the model at the quarter span location to simulate the effect of loading on the bridge, as shown in Figure 18. The damage Scenario 2 is studied with unsymmetrical damage locations in two girders to investigate if the sensitivity could be improved and the detection on the undamaged locations SB1 and SB8 in the opposite girder could be influenced. The ambient tests are performed in the undamaged and damaged states with the mass blocks on the structure. Figure 19 shows the damage detection results and indicates that the introduced damage locations are clearly identified. Compared with the detection results without mass in Figure 19(a), the detection with mass blocks on the model shown in Figure 19(b) has much higher damage index values without false identifications on the

Figure 18. The testing model with mass blocks

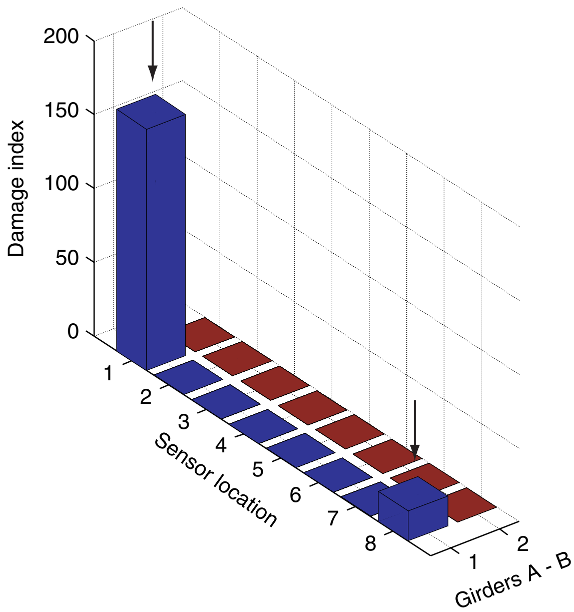

(b) With mass

Figure 19. *(Continued)*

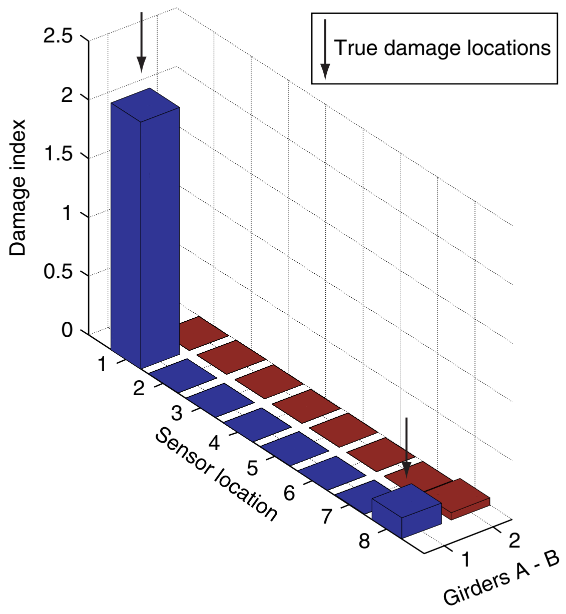

(a) Without mass

Figure 19. Comparison of damage detection results without and with mass blocks

opposite locations SB1 and SB8 in girder B and indicates that the proposed method is quite sensitive to identify the damages of shear connectors in composite bridges when the bridge is subject to loads.

6. CONCLUSIONS

This paper proposes a dynamic condition assessment approach based on wavelet packet energy of cross-correlation functions of measured acceleration responses under ambient excitations to identify the damage of shear connectors in composite bridge structures, such as slab-on-girder structures. Measured acceleration responses on the slab and corresponding girder locations in the undamaged and damaged states are used to compute the cross-correlation functions. Wavelet packet decomposition of the cross-correlation functions is performed. The percentage of wavelet packets energy to the total wavelet packet energy, as a function of system's impulse response functions, can be used for damage detection. The energy percentage of selected wavelet packets with specific frequency bandwidths in the undamaged and damaged states is used to detect the damage locations of shear connectors. Numerical and experimental studies on a composite bridge with a concrete slab supported on two steel girders are conducted to validate the accuracy and investigate the performance and robustness of the approach with noisy measurements. Two damage scenarios are assumed, and identification results from simulated noisy responses under different ambient excitation levels in the numerical study show that the damage of shear connectors can be identified effectively even with 10% noise in the measured responses. The proposed approach has a good robustness and performance. The measured acceleration responses from a composite bridge in the laboratory under ambient vibrations are used to identify the shear connector damage. Repeated tests can be performed with a limited number of sensors to eliminate the constraint of sensor numbers. It is demonstrated that the introduced damage locations of shear connectors can be identified accurately even the ambient vibration level in the laboratory is quite small. A few false positives may exist in the identified results due to the low signal to noise ratio and smearing effect in the damage detection.

Global modal information, such as COMAC and changes in flexibility, may not be sensitive enough to be a good indicator to detect the damage of shear connectors. The focus of this paper is to achieve a condition assessment approach to identify the shear connector conditions with ambient vibration measurements and detect the possible existence of shear link damage. It is difficult to perform the tests with different damage states of shear connectors. If a shear link or a bolt in this study is not completely removed, to create relative movement between deck and girder, large shear deformation of the bolt or concrete crushing damage around bolt needs to be induced. Such damage could occur in a real bridge under traffic loading, but it is not likely in the lab tests under low ambient excitations. This is the limitation of the tests. The detection with a single damaged shear connector has been tried but the damage could not be reliably identified. This is because the ambient excitation level in the experimental study is quite low, basically in a quiet lab with the test model placed on a strong floor. If the vibration level is very low, friction resistance plus the undamaged shear links between deck and girder is sufficient to resist relative movement between deck and girder. The friction resistance acts the same as the shear links. Therefore the shear link damage cannot be reliably identified. The shear link damage can be reliably identified only if the vibration level is large enough to overcome the friction resistance. Therefore the method is expected to give better damage identifications in a real bridge under traffic loading. Studies on the condition assessment of shear connectors in real bridge structures under traffic loads with in-field testing data will be conducted.

ACKNOWLEDGMENTS

The work described in this paper was supported by "Supporting Infrastructure Management by Combining Sensors and Asset Information Models - Project No. 3104", Australia Cooperative Research Centre for Infrastructure and Engineering Asset Management (CIEAM-II), and Australian Research Council Discovery Early Career Researcher Award DE140101741, "Development of a Self-powered Wireless Sensor Network from Renewable Energy for Integrated Structural Health Monitoring and Diagnosis".

REFERENCES

Akansu, A.N. and Haddad, R.A. (1992). *Multiresolution Signal Decomposition: Transforms, Subbands, Wavelets*, New York: Academic.

Bendat, J.S. and Piersol, A.G. (1980). *Engineering Applications of Correlation and Spectral Analysis*, John Wiley & Sons, USA.

Bernal, D., and Gunes, B. (2004). "Flexibility based approach for damage characterization: benchmark application", *Journal of Engineering Mechanics*, ASCE, Vol. 130, No. 1, pp. 61–70.

Brincker, R., Zhang, L. and Andersen, P. (2000). "Modal identification from ambient responses using frequency domain decomposition", *Proceedings, IMAC-XVIII: A Conference on Structural Dynamics*, San Antonio, TX, pp. 625–630.

Brownjohn, J.M.W., Dumanoglu, A.A. and Severn, R.T. (1992). "Ambient vibration survey of the fatih sultan mehmet (second Bosporus) suspension bridge", *Earthquake Engineering and Structural Dynamics*, Vol. 21, No. 10, pp. 907–924.

Chiewanichakorn, M., Aref, A.J., Chen, S.S. and Ahn, S. (2004). "Effective flange width definition for steel-concrete composite bridge girder", *Journal of Structural Engineering*, ASCE, Vol. 130, No. 12, pp. 2016–2031.

De Roeck, G., Peeters, B. and Ren, W.X. (2000). "Benchmark study on system identification through ambient vibration measurements", *Proceedings, IMAC-XVIII: The 18th International Modal Analysis Conference*, San Antonio, TX, pp. 1106–1112.

Dilena, M. and Morassi, A. (2003). "A damage analysis of steel-concrete composite beams via dynamic methods: Part II. analytical models and damage detection", *Journal of Vibration and Control*, Vol. 9, No. 5, pp. 529–565.

Dilena, M. and Morassi, A. (2004). "Experimental modal analysis of steel concrete composite beams with partially damaged connection", *Journal of Vibration and Control*, Vol. 10, No. 6, pp. 897–913.

Duan, Z., Yan, G., Ou, J. and Spencer, B.F. (2007). "Damage detection in ambient vibration using proportional flexibility matrix with incomplete measured DOFs", *Structural Control and Health Monitoring*, Vol. 14, No. 2, pp. 186–196.

Fryba, L. and Pirner, M. (2001). "Load tests and modal analysis of bridges", *Engineering Structures*, Vol. 23, No. 1, pp. 102–109.

Hamey, C.S., Lestari, W., Qiao, P. and Song, G. (2004). "Experimental damage identification of carbon/epoxy composite beams using curvature mode shapes", *Structural Health Monitoring*, Vol. 3, No. 4, pp. 333–353.

Han, J.G., Ren, W.X. and Sun, Z.S. (2005). "Wavelet packet based damage identification of beam structures", *International Journal of Solids and Structures*, Vol. 42, No. 26, pp. 6610–6627.

Lee, J.J. and Yun, C.B. (2006). "Damage diagnosis of steel girder bridges using ambient vibration data", *Engineering Structures*, Vol. 28, No. 6, pp. 912–925.

Lieven, N.A.J. and Ewins, D.J. (1988). "Spatial correlation of mode shapes, the co-ordinate Modal Assurance Criterion (COMAC)", *Proceedings, The 6th International Modal Analysis Conference*, Orlando, Florida, Vol. 1, pp. 690–695.

Liu, K. and De Roeck, G. (2009). "Damage detection of shear connectors in composite bridges", *Structural Health Monitoring*, Vol. 8, No. 5, pp. 345–356.

Morassi, A. and Rocchetto, L. (2003). "A damage analysis of steel-concrete composite beams via dynamic methods: Part I. experimental results", *Journal of Vibration and Control*, Vol. 9, No. 5, pp. 507–527.

Newmark, N.W. (1959). "A method of computation for structural dynamics", *Journal of Engineering Mechanics Division*, ASCE, Vol. 85, No. 3, pp. 67–94.

Pandey, A.K. and Biswas, M. (1994). "Damage detection in structures using changes in flexibility", *Journal of Sound and Vibration*, Vol. 169, No. 1, pp. 3–17.

Ren, W.X., Sun, Z.S., Xia, Y., Hao, H. and Deeks, A.J. (2008). "Damage identification of shear connectors with wavelet packet energy: laboratory test study", *Journal of Structural Engineering*, ASCE, Vol. 134, No. 5, pp. 832–841.

Salawu, O.S. (1997). "Detection of structural damage through changes in frequency: a review", *Engineering Structures*, Vol. 19, No. 9, pp. 718–723.

Samali, B., Dackermann, U. and Li, J. (2012). "Location and severity identification of notch-type damage in a two-storey steel framed structure utilising frequency response functions and artificial neural network", *Advances in Structural Engineering*, Vol. 15, No. 5, pp. 743–758.

Shi, Z.Y., Law, S.S. and Zhang, L.M. (2000). "Structural damage detection from modal strain energy change", *Journal of Engineering Mechanics*, ASCE, Vol. 126, No. 12, pp. 1216–1223.

Sun, Z. and Chang, C.C. (2004). "Statistical wavelet-based method for structural health monitoring", *Journal of Structural Engineering*, ASCE, Vol. 130, No. 7, pp. 1055–1062.

Wu, W., Chen, C. and Liau, J. (2012). "A multiple random decrement method for modal parameter identification of stay cables based on ambient vibration signals", *Advances in Structural Engineering*, Vol. 15, No. 6, pp. 969–982.

Xia, Y., Hao, H. and Deeks, A.J. (2007). "Dynamic assessment of shear connectors in slab-girder bridges", *Engineering Structures*, Vol. 29, No. 7, pp. 1457–1486.

Xia, Y., Hao, H., Deeks, A.J. and Zhu, X.Q. (2008). "Condition assessment of shear connectors in slab-girder bridges via vibration measurements", *Journal of Bridge Engineering*, ASCE, Vol. 13, No. 1, pp. 43–54.

Yen, G.G. and Lin, K.C. (2000). "Wavelet packet feature extraction for vibration monitoring", *IEEE Transactions on Industrial Electronics*, Vol. 47, No. 3, pp. 650–667.

Yuen, K.V. and Katafygiotis, L.S. (2003). "Bayesian fast Fourier transform approach for model updating using ambient data", *Advances in Structural Engineering*, Vol. 6, No. 2, pp. 81–95.

Zhu, X.Q., Hao, H., Uy, B., Xia, Y. and Mirza, O. (2012). "Dynamic assessment of shear connection conditions in slab-girder bridges by Kullback-Leibler distance", *Advances in Structural Engineering*, Vol. 15, No. 5, pp. 771–780.